Physicochemical properties of pentaglyme–sodium bis(trifluoromethanesulfonyl)amide solvate ionic liquid

ARTICLE *in* PHYSICAL CHEMISTRY CHEMICAL PHYSICS · MAY 2014

Impact Factor: 4.49 · DOI: 10.1039/c4cp00746h · Source: PubMed

8 AUTHORS, INCLUDING:

Toshihiko Mandai
Chalmers University of Technology
27 PUBLICATIONS **250** CITATIONS
SEE PROFILE

Kazuhide Ueno
Yamaguchi University
69 PUBLICATIONS **1,244** CITATIONS
SEE PROFILE

Kaoru Dokko
Yokohama National University
140 PUBLICATIONS **3,021** CITATIONS
SEE PROFILE

Masayoshi Watanabe
Yokohama National University
350 PUBLICATIONS **14,344** CITATIONS
SEE PROFILE

Lithium Ion Solvation in Room-Temperature Ionic Liquids Involving Bis(trifluoromethanesulfonyl) Imide Anion Studied by Raman Spectroscopy and DFT Calculations

Yasuhiro Umebayashi, Takushi Mitsugi, Shuhei Fukuda, Takao Fujimori, Kenta Fujii, Ryo Kanzaki, Munetaka Takeuchi, and Shin-Ichi Ishiguro*

Department of Chemistry, Faculty of Science, Kyushu University, Hakozaki, Higashi-ku, Fukuoka, 812-8581, Japan

Received: August 28, 2007

The solvation structure of the lithium ion in room-temperature ionic liquids 1-ethyl-3-methylimidazolium bis(trifluoromethanesulfonyl) imide (EMI^+TFSI^-) and *N*-butyl-*N*-methylpyrrolidinium bis(trifluoromethanesulfonyl) imide (BMP^+TFSI^-) has been studied by Raman spectroscopy and DFT calculations. Raman spectra of EMI^+TFSI^- and BMP^+TFSI^- containing Li^+TFSI^- over the range 0.144−0.589 and 0.076−0.633 mol dm^{-3}, respectively, were measured at 298 K. A strong 744 cm^{-1} band of the free $TFSI^-$ ion in the bulk weakens with increasing concentration of the lithium ion, and it revealed by analyzing the intensity decrease that the two $TFSI^-$ ions bind to the metal ion. The lithium ion may be four-coordinated through the O atoms of two bidentate $TFSI^-$ ions. It has been established in our previous work that the $TFSI^-$ ion involves two conformers of C_1 (*cis*) and C_2 (*trans*) symmetries in equilibrium, and the dipole moment of the C_1 conformer is significantly larger than that of the C_2 conformer. On the basis of these facts, the geometries and SCF energies of possible solvate ion clusters $[Li(C_1\text{-}TFSI^-)_2]^-$, $[Li(C_1\text{-}TFSI^-)(C_2\text{-}TFSI^-)]^-$, and $[Li(C_2\text{-}TFSI^-)_2]^-$ were examined using the theoretical DFT calculations. It is concluded that the C_1 conformer is more preferred to the C_2 conformer in the vicinity of the lithium ion.

Introduction

Lithium is used as a material for ubiquitous power sources, not only an electrolyte for secondary batteries but also a polymer or solid electrolyte. Solvation of the lithium ion has thus been investigated in aqueous solution,[1] as well as nonaqueous solution in view of the structure[2] and dynamics.[3] Recently, room-temperature ionic liquids (RTILs) have been paid increasing attention as new solvents of negligible vapor pressure and incombustibility. Indeed, 1-ethyl-3-methylimidazolium bis(trifluoromethanesulfonyl) imide (EMI^+TFSI^-) ionic liquid is used for a solvent of lithium ion secondary batteries.[4] However, the EMI^+ ionic liquids show a relatively narrow electrochemical window for lithium ion secondary batteries. As alternatives, cyclic quaternary ammonium ions,[5] quaternary ammonium ions with a cyano group,[6] and 1-butyl-2,3-dimethylimidazolium,[7] diethylmethyl(methoxyethyl)ammonium ($DEME^+$),[8] and aliphatic onium cations[9] were proposed.

Molecular geometries in RTILs have been studied, and it has been established that RTILs involve conformers and the conformational change plays an essential role in their structure and dynamics.[10] We found two EMI^+ conformers, in which the ethyl group locates planar *cis* or nonplanar staggered against the imidazolium ring,[11] and two $TFSI^-$ conformers with the C_1 (*cis*) and C_2 (*trans*) symmetries,[12] and conformational equilibria are established between them. The *N*-butyl-*N*-methylpyrrolidinium (BMP^+) bis(trifluoromethanesulfonyl) imide involves BMP^+ conformers in equilibrium, in which the butyl group locates *axially* or *equatorially* against the *envelope* pyrrolidinium ring.[13] The conformational equilibrium for EMI^+ is supported by molecular dynamics (MD) simulations according to Lopes et al.[14] It is also supported by large-angle neutron scattering (LANS) and MD simulations for $TFSI^-$ in 1,3-dimethylimidazolium bis(trifluoromethanesulfonyl) imide ionic liquid,[15] as well as in nonaqueous solution[16] and tetraethylammonium bis(trifluoromethanesulfonyl) imide at elevated temperature.[17]

The solvation structure of the lithium ion has been studied,[18] as it plays an essential role in the ion conductivity and charge−discharge reactivity in the battery. Hagiwara et al. reported the crystal structure of $Li^+_2(EMI^+)(TFSI^-)_3$.[19] Raman and NMR spectroscopic studies were reported for the mixture of *N*-methyl-*N*-propylpyrrolidinium bis(trifluoromethanesulfonyl) imide and Li^+TFSI^- over a wide temperature range by Henderson and Passerini et al.[20] Borodin and Smith et al. investigated lithium ion solvation in some *N*-methyl-*N*-alkylpyrrolidinium bis(trifluoromethanesulfonyl) imide ionic liquids by MD simulations.[21] Recently, Hardwick et al. studied by Raman spectra lithium ion solvation in mixtures of EMI^+TFSI^- and some carbonates.[22] Lassègues et al. proposed that two $TFSI^-$ ions coordinate to the lithium ion to change the conformation.[23] However, information on the solvation structure of the lithium ion in ionic liquids is still limited. In the present work, we thus report the solvation structure of the lithium ion in RTILs EMI^+TFSI^- and BMP^+TFSI^- studied by Raman spectroscopy and DFT calculations.

Experimental Section

Materials. EMI^+TFSI^- and BMP^+TFSI^- of spectroscopic grade (Japan Carlite Co. Ltd.) were used without further purification. The water content was checked by a Karl Fischer

* To whom correspondence should be addressed. E-mail: analsscc@mbox.nc.kyushu-u.ac.jp.

10.1021/jp076869m CCC: $37.00
Published on Web 10/19/2007

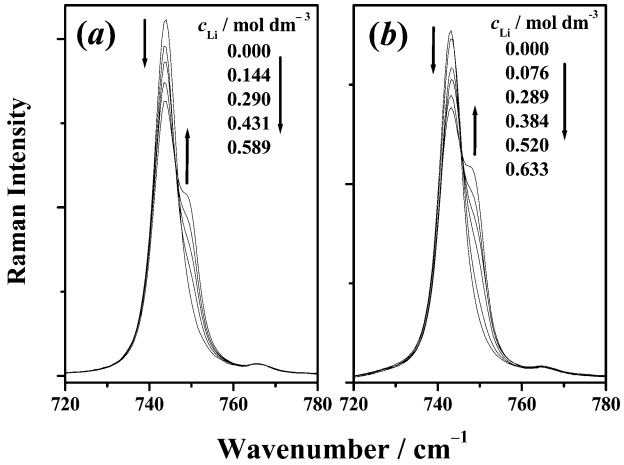

Figure 1. Raman spectra of EMI$^+$TFSI$^-$ containing 0.144, 0.290, 0.431, and 0.589 mol dm^{-3} Li$^+$TFSI$^-$ (a) and BMP$^+$TFSI$^-$ containing 0.076, 0.289, 0.384, 0.520, and 0.633 mol dm^{-3} Li$^+$TFSI$^-$ (b). In both panes, Raman spectra of the neat ionic liquids are also shown.

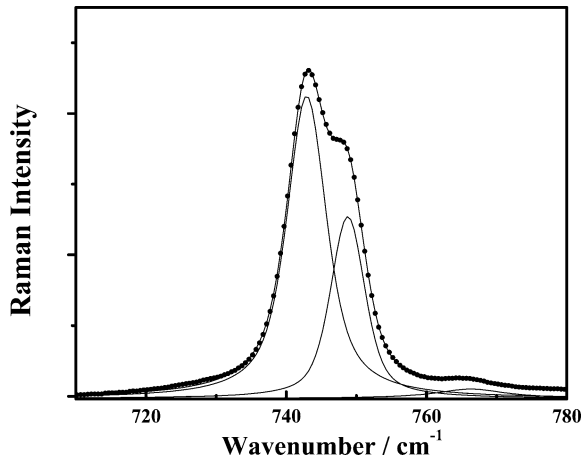

Figure 2. Deconvoluted Raman spectrum of an EMI$^+$TFSI$^-$ solution containing 0.589 mol dm^{-3} Li$^+$TFSI$^-$ over the range 720−780 cm^{-1}. Observed and calculated Raman spectra (the dotted and solid lines, respectively) and the deconvoluted bands (the solid lines) of free TFSI$^-$ (744 cm^{-1}), bound TFSI$^-$ (750 cm^{-1}), and EMI$^+$ (766 cm^{-1}) are shown.

test to be less than 60 ppm. Li$^+$TFSI$^-$ salts (Morita) were dried in vacuo at 425 K for 1 day and used without further purification. All materials were treated in a high-performance glovebox (Miwa), in which the water and oxygen contents were kept at less than 1 ppm.

Raman Spectroscopy. Sample solutions were prepared by dissolving a given amount of Li$^+$TFSI$^-$ crystals in each ionic liquid. Raman spectra were obtained using an FT-Raman spectrometer (Perkin-Elmer GX-R) equipped with a Nd:YAG laser operating at 1064 nm. The laser power was kept at 800 mW throughout the measurements. The optical resolution was 2.0 cm^{-1}, and spectral data were accumulated 1024 times to obtain data of a sufficiently high signal-to-noise ratio. The sample liquid in a quartz cell was stirred and thermostated at a given temperature within ±0.3 K. No appreciable damage of the sample was detected after irradiation. Measured Raman intensities were normalized using the 960 cm^{-1} (EMI$^+$) and 825 cm^{-1} (BMP$^+$) bands,[11,13] and the concentration of the ions in the sample solutions were corrected for density. The densities of the sample solutions were measured using a densimeter (Kyoto Electronics DA 300).

Raman spectra were deconvoluted to extract single Raman bands. A single Raman band is assumed to be represented as a

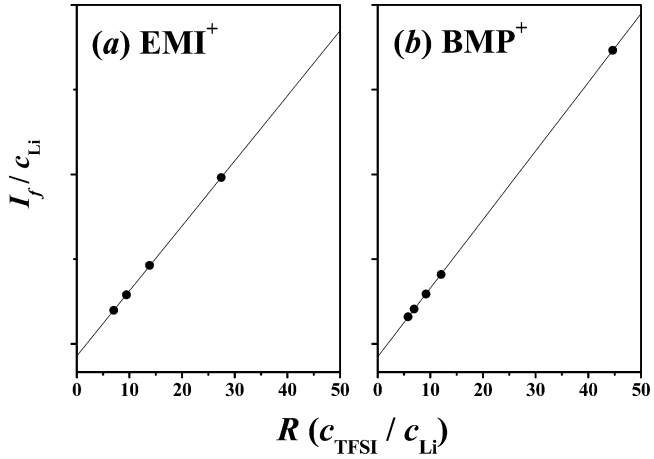

Figure 3. I_f/c_{Li} plots vs R for EMI$^+$TFSI$^-$ (a) and BMP$^+$TFSI$^-$ (b).

CHART 1: Optimized Geometries of the [Li(C_1-TFSI$^-$)$_2$]$^-$, [Li(C_1-TFSI$^-$)(C_2-TFSI$^-$)]$^-$, and [Li(C_2-TFSI$^-$)$_2$]$^-$ Ion Clusters Calculated Using the B3LYP/6-311+G(d) Level of Theory

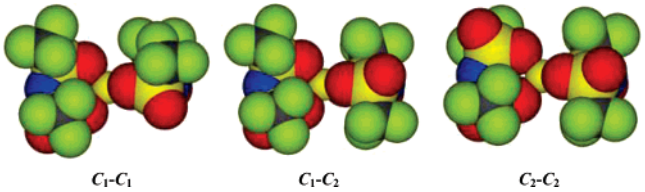

pseudo-Voigt function, $f_V(\nu) = \gamma f_L(\nu) + (1 - \gamma) f_G(\nu)$, where $f_L(\nu)$ and $f_G(\nu)$ stand for the Lorentzian and Gaussian components, respectively, and the parameter γ ($0 < \gamma < 1$) is the fraction of the Lorentzian component. To avoid uncertainty in obtaining the γ value of the peaks, the value was fixed to that obtained at the highest lithium ion concentration. The intensity I of a single Raman band is evaluated according to $I = \gamma I_L + (1 - \gamma) I_G$, where I_L and I_G denote the integrated intensities of the Lorentzian and Gaussian components, respectively. A nonlinear least-squares curve-fitting program, based on the Marquardt−Levenberg algorithm,[24,25] was developed in our laboratory and used throughout the analyses.

DFT Calculations. The TFSI$^-$ ion involves two conformers of C_1 (*cis*) and C_2 (*trans*) symmetries. The geometry optimization and normal coordinate analyses were carried out for the 1:1 and 1:2 Li−TFSI$^-$ ion clusters by taking into account the conformation of the anion on the basis of density functional theory according to Becke's three-parameter hybrid method[26] with LYP correlation (B3LYP)[27] and the relatively large basis set with diffuse and polarization functions, 6-311+G(d). The basis set superposition errors (BSSEs) were checked to be negligible by the counterpoise method.[28] DFT calculations were carried out using the Gaussian03 program package.[29]

Results and Discussion

Solvation Number of the Lithium Ion. Raman spectra of liquid EMI$^+$TFSI$^-$ and BMP$^+$TFSI$^-$ were measured over the frequency range 200−1700 cm^{-1}. It has been established that the TFSI$^-$ ion involves the C_1 and C_2 conformers in equilibrium, in which two CF_3 groups locate *cis* and *trans*, respectively, within the CF_3−S−N−S−CF_3 skeleton.[12] Raman spectra of these conformers are very similar to give an overlapped intense band at 744 cm^{-1}, which is ascribed to the CF_3 bending vibration $\delta_s(CF_3)$ coupled with the S−N stretching vibration ν_s(SNS).[30] However, as seen in Figure 1, a new band appears at the higher

TABLE 1: Average Bond Lengths, Bond Angles, and Dihedral Angles and Binding Energies ΔE for the Optimized Geometries of the $[Li(C_1\text{-}TFSI^-)_2]^-$, $[Li(C_1\text{-}TFSI^-)(C_2\text{-}TFSI^-)]^-$, and $[Li(C_2\text{-}TFSI^-)_2]^-$ Ion Clusters Calculated Using the B3LYP/6-311+G(d) Level of Theory

		$[Li(C_1\text{-}TFSI^-)(C_2\text{-}TFSI^-)]^+$		
	$[Li(C_1\text{-}TFSI^-)_2]^+$	C_1	C_2	$[Li(C_2\text{-}TFSI^-)_2]^+$
		Bond Lengths r/Å		
Li^+-O	1.951	1.947		1.946
N−S	1.605	1.605	1.605	1.605
S−O	1.465	1.465	1.464	1.465
S−C	1.892	1.892	1.890	1.890
C−F	1.337	1.337	1.337	1.337
		Bond Angles θ/deg		
Li^+-O-S	132.5	132.9	133.5	133.4
$O-Li^+-O$ (intra)	92.7	92.7		92.7
$O-Li^+-O$ (inter)	118.4	118.4		118.4
S−N−S	126.0	126.2	125.9	125.9
N−S−O	112.7	112.7	113.0	113.0
N−S−C	103.1	103.3	101.8	101.7
O−S−C	104.0	103.9	104.2	104.3
O−S−O	118.2	118.2	118.2	118.1
S−C−F	110.2	110.2	110.2	110.2
F−C−F	108.7	108.7	108.8	108.8
		Dihedral Angles ϕ/deg		
S−N−S−C	98	99	103	103
S−N−S−C	−120	−119		
ΔE/kJ mol^{-1}	−792.5	−791.2		−788.9

frequency side of the 744 cm^{-1} band upon the addition of Li^+TFSI^- to the ionic liquids, which is in agreement with the result in the litereature.[20,22,23] The new band is intensified with increasing metal ion concentration, whereas the 744 cm^{-1} band weakens to show a pseudoisosbestic point. For EMI^+TFSI^- solutions containing Li^+TFSI^-, observed Raman spectra in the range 720−780 cm^{-1} were satisfactorily deconvoluted into three bands at 744, 750, and 767 cm^{-1}, as shown in Figure 2. The same bands were also extracted for BMP^+TFSI^- solutions. The new band at 750 cm^{-1} is ascribed to the $TFSI^-$ ion bound to the lithium ion, the vibrational mode of which corresponds to the 744 cm^{-1} band of the free $TFSI^-$ ion.[30a,31] Weak and overlapped bands appearing at around 767 cm^{-1} may be ascribed to the cation and anion. According to our previous Raman spectroscopic study and quantum calculations, the EMI^+ and BMP^+ ions show no significant Raman band in the range 720−760 cm^{-1};[11,13] i.e., no spectral contamination is expected for the 744 cm^{-1} band of $TFSI^-$. Therefore, the solvation number, or the number of $TFSI^-$ ions bound to the lithium ion, is evaluated by analyzing integrated intensities of the extracted 744 cm^{-1} bands by deconvolution.

The integral intensity I_f of an extracted band of the free $TFSI^-$ ion is given as $I_f = J_f c_f$, where J_f and c_f stand for the molar Raman scattering coefficient and the concentration of the $TFSI^-$ ion in the bulk, respectively. c_f is given as $c_f = c_T - c_b = c_T - nc_{Li}$, where c_T, c_b, c_{Li}, and n denote the concentrations of total and bound $TFSI^-$ ions and the concentration and solvation number of the lithium ion, respectively. By inserting the equation into $I_f = J_f c_f$, we obtain the following relationship: $I_f/c_{Li} = J_f(R - n)$, where $R = c_T/c_{Li}$. The plot of I_f/c_{Li} against R thus gives a straight line, and the n value is obtained as $n = -\beta/\alpha$ from the slope $\alpha = J_f$ and the intercept $\beta = -J_f n$. The plots for the 744 cm^{-1} band obtained for EMI^+TFSI^- and BMP^+TFSI^- are shown in Figure 3. The solvation number was evaluated to be 1.86(8) and 1.86(3) in EMI^+TFSI^- and BMP^+TFSI^-, respectively, which indicates that two $TFSI^-$ ions bind to the lithium ion in both ionic liquids, if we take into account experimental errors. The result is in good agreement with the that reported by Lassègues et al.[23] It has been established that the lithium ion prefers a tetrahedrally 4-coordinated structure with O donor ligands in aqueous and nonaqueous solutions.[1,2,17] It is thus plausible that the $TFSI^-$ ion binds to the lithium ion as a bidentate O donor ligand in the ionic liquids. Indeed, according to ab initio calculations for the Li^+TFSI^- ion pair,[32] the lithium ion is coordinated with two sulfonyl groups through the O atom.

The relationship $I_b = J_b c_b = J_b n c_{Li}$ holds also for the $TFSI^-$ ion bound to the lithium ion, and the molar scattering coefficient J_b is obtained from the I_b vs c_{Li} plot for the 750 cm^{-1} band. The ratio J_b/J_f obtained in this study is 0.9 for both ionic liquids. The J_b value similar to J_f implies that the $TFSI^-$ ion is not strongly polarized in the coordination sphere of the lithium ion.

DFT Calculations. The $TFSI^-$ ion involves two sulfonyl groups, which bind to the lithium ion through the O atom. According to Gejji et al.,[32b] the binding energy of the $Li^+(C_1\text{-}TFSI^-)$ ion pair is practically the same as that of the $Li^+(C_2\text{-}TFSI^-)$ ion pair. However, the lithium ion binds two $TFSI^-$ ions in both EMI^+TFSI^- and BMP^+TFSI^- ionic liquids. Therefore, by taking into account the solvation number and conformation of the $TFSI^-$ ion, we carried out DFT calculations for three possible ion clusters, $[Li(C_1\text{-}TFSI^-)_2]^-$ (C_1-C_1), $[Li(C_1\text{-}TFSI^-)(C_2\text{-}TFSI^-)]^-$ (C_1-C_2), and $[Li(C_2\text{-}TFSI^-)_2]^-$ (C_2-C_2). The optimized geometries with no imaginary frequency were successfully obtained for all the solvate ions and are shown in Chart 1.

The SCF energy E_{SCF} is the lowest for the C_2-C_2 cluster. The relative SCF energy ΔE_{SCF} ($= E_{SCF}$(cluster) $- E_{SCF}(C_2-C_2)$) is 1.0 kJ mol^{-1} for the C_1-C_1 cluster and 0.0 kJ mol^{-1} for the C_1-C_2 cluster, indicating that the SCF energy hardly depends on the conformation of $TFSI^-$. The binding energy is then calculated according to $\Delta E = E_{SCF}$(cluster) $- E_{SCF}(Li^+) - 2E_{SCF}(TFSI^-)$. The values thus calculated are −792.5, −791.2, and −788.9 kJ mol^{-1} for the C_1-C_1, C_1-C_2, and C_2-C_2 ion clusters, respectively. According to Tsuzuki et al.,[33] the value for C_2-C_2 calculated using the MP2/6-311G(d,p)//HF/6-311G(d,p) level of theory is −761.5 kJ mol^{-1}, which is in good agreement with ours. The binding energy is appreciably larger for C_1-C_1 than C_2-C_2. This might be ascribed to the larger dipole moment (4.404 D) of the C_1 conformer than that (0.301 D) of the C_2 conformer.[12] However, note that the

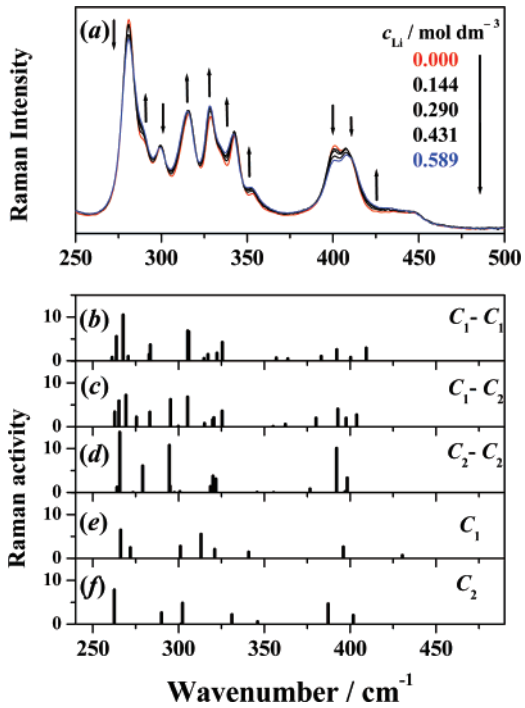

Figure 4. Observed Raman spectra of EMI^+TFSI^- (a) and theoretical spectra for the optimized geometries of $[Li(C_1\text{-}TFSI^-)_2]^-$ (b), $[Li(C_1\text{-}TFSI^-)(C_2\text{-}TFSI^-)]^-$ (c), and $[Li(C_2\text{-}TFSI^-)_2]^-$ (d). Theoretical Raman spectra for the C_1 (e) and the C_2 (f) isomers of $TFSI^-$ are also shown.

corresponding ΔE values for the 1:1 Li^+TFSI^- ion pair obtained using the same level of theory are -601.3 and -604.6 kJ mol^{-1} for the C_1 and the C_2 conformers, respectively, indicating that the C_1 conformer is still rather disfavored around the lithium ion in the 1:1 ion pair, like in the bulk. This implies that a specific interaction other than the ion−dipole interaction plays a role in the larger binding energy of the C_1-C_1 ion cluster than that of C_2-C_2. Selected structural parameters and binding energies are listed in Table 1. No significant structural change is found for the intramolecular structure of the $TFSI^-$ ion in all the solvates. The predicted Li^+-O ($TFSI^-$) bond length is 1.951, 1.947, and 1.946 Å for the C_1-C_1, C_1-C_2, and C_2-C_2 ion clusters, respectively. The bond length is longer for C_1-C_1 than that for C_2-C_2, which is unexpected because the binding energy of C_1-C_1 is larger than that of C_2-C_2, as noted above. Indeed, the Li−O (ligand) bond length in crystals of four-coordinated complexes decreases in the order ethers (1.962 Å), water (1.944 Å), amides (1.923 Å), and carboxylates (1.957 Å),[34] the order of increasing electron pair donating ability. This also implies that a specific interaction operates within the C_1-C_1 ion clusters.

Conformation of the $TFSI^-$ Ion around the Lithium Ion. According to Lassègues et al.,[35] Raman spectra over the frequency range 250−500 cm^{-1} well reflect the conformational change of the $TFSI^-$ ion. Figure 4a shows observed Raman spectra of EMI^+TFSI^- containing various concentrations of Li^+TFSI^- over the frequency range. As seen, the bands at 288, 315, 328, 343, and 353 cm^{-1} are intensified with increasing concentration of the lithium ion, whereas the 279, 297, 396, and 406 cm^{-1} bands are weakened, and besides, a new band appears at around 420 cm^{-1}. This fact indicates that the $TFSI^-$ ion changes its conformation upon solvation to the lithium ion, as pointed out by Lassègues et al.[23] Also for BMP^+TFSI^-, both 396 and 406 cm^{-1} bands weaken with increasing concentration of the lithium ion, but the extent is more marked for the former. The same aspect is seen with increasing temperature,[11,13] and here, according to the van't Hoff equation, the population of the C_1 conformer increases, as the enthalpy of the conformational change from C_2 to C_1 is positive (3.5 kJ mol^{-1}).[12] This leads to the conclusion that the population of the C_1 conformer increases with increasing concentration of the lithium ion or the C_1 conformer is preferred in the vicinity of the lithium ion. We thus conclude that the enhanced and weakened Raman bands are ascribed to the C_1 and C_2 conformers, respectively. The same conclusion is also drawn from DFT calculations. Predicted Raman bands for the C_1-C_1, C_1-C_2, and C_2-C_2 ion clusters are shown in Figure 4, together with those of the single C_1 and C_2 conformers. These calculated normal frequencies, Raman activities, and IR intensities for the ion clusters are listed in Table S1 in the Supporting Information. The enhanced bands at 315, 328, 343, and 406 cm^{-1} are evidently ascribed to the C_1-C_1 and C_1-C_2 ion clusters, whereas the weakened band at 396 cm^{-1} is ascribed to the C_2-C_2 ion cluster.

To conclude, it has been established that the C_1 (*cis*) conformer is preferred to the C_2 (*trans*) conformer in the vicinity of the lithium ion, unlike in the bulk. The C_1 conformer is also preferred in $Li^+{}_2(EMI^+)(TFSI^-)_3$ crystals,[19] as well as in $AE(Tf_2N)_4^{2-}$ (AE = Ca^{2+}, Sr^{2+}, and Ba^{2+}) crystals.[36] However, distribution of conformers in the vicinity of the lithium ion is not revealed yet. Further information on the Gibbs energy, enthalpy, and entropy values of the conformational change of the $TFSI^-$ ion in the vicinity of the lithium ion is needed to clarify the solvation of the metal ion in the ionic liquid.

Acknowledgment. This work has been financially supported by Grants-in-Aid for Scientific Research, Nos. 17350037, 18850017, 19350033, and 19750062, from the Ministry of Education, Culture, Sports, Science and Technology.

Supporting Information Available: Observed Raman spectra of EMI^+TFSI^- and BMP^+TFSI^- ionic liquids containing Li^+TFSI^- (Figures S1 and S2, respectively) and theoretical IR/Raman spectra (Table S1). This material is available free of charge via the Internet at http://pubs.acs.org.

References and Notes

(1) (a) Kameda, Y.; Sasaki, M.; Amo, Y.; Usuki, T. *Bull. Chem. Soc. Jpn.* **2006**, *79*, 228−236. (b) Kameda, Y.; Mochiduki, K.; Imano, M.; Naganuma, H.; Sasaki, M.; Amo, Y.; Usuki, T. *J. Mol. Liq.* **2005**, *119*, 159−166. (c) Kameda, Y.; Imano, M.; Takeuchi, M.; Suzuki, S.; Usuki, T.; Uemura, O. *J. Non-Cryst. Solids* **2001**, *293*−*295*, 600−606. (d) Kameda, Y.; Ebata, H.; Uemura, O. *Bull. Chem. Soc. Jpn.* **1994**, *67*, 929−935. (e) Kameda, Y.; Uemura, O. *Bull. Chem. Soc. Jpn.* **1993**, *66*, 384−389.

(2) (a) Burba, C. M.; Frech, R. *J. Phys. Chem. B* **2005**, *109*, 15161−15164. (b) Brouillette, D.; Irish, D. E.; Taylor, N. J.; Perron, G.; Odziemkowski, M.; Desnoyers, J. E. *Phys. Chem. Chem. Phys.* **2002**, *4*, 6063−6071. (c) Caillon-Caravanier, M.; Bosser, G.; Claude-Montigny, B.; Lemordant, D. *J. Electrochem. Soc.* **2002**, *149*, E340−E347. (d) Wang, Z.; Gao, W.; Huang, X.; Mo, Y.; Chen, L. *J. Raman Spectrosc.* **2001**, *32*, 900−905. (e) Barthel, J.; Buchner, R.; Wismeth, E. *J. Solution Chem.* **2000**, *29*, 937−954. (f) Aroca, R.; Nazri, M.; Nazri, G. A.; Camargo, A. J.; Trsic, M. *J. Solution Chem.* **2000**, *29*, 1047−1060. (g) Klassen, B.; Aroca, R.; Nazri, M.; Nazri, G. A. *J. Phys. Chem. B* **1998**, *102*, 4795−4801. (h) Morita, M.; Asai, Y.; Yoshimoto, N.; Ishikawa, M. *J. Chem. Soc., Faraday Trans.* **1998**, *94*, 3451−3456. (i) Kameda, Y.; Kudoh, N.; Suzuki, S.; Usuki, T. i.; Uemura, O. *Bull. Chem. Soc. Jpn.* **2001**, *74*, 1009−1014. (j) Kameda, Y.; Ebata, H.; Usuki, T.; Uemura, O. *Physica B (Amsterdam)* **1995**, *213*, *214*, 477−479.

(3) (a) Hayamizu, K.; Seki, S.; Miyashiro, H.; Kobayashi, Y. *J. Phys. Chem. B* **2006**, *110*, 22302−22305. (b) Hayamizu, K.; Aihara, Y. *Electrochim. Acta* **2004**, *49*, 3397−3402. (c) Aihara, Y.; Bando, T.; Nakagawa, H.; Yoshida, H.; Hayamizu, K.; Akiba, E.; Price, W. S. *J. Electrochem. Soc.* **2004**, *151*, A119−A122. (d) Hayamizu, K.; Akiba, E. *Electrochemistry* **2003**, *71*, 1052−1054. (e) Hayamizu, K.; Akiba, E.; Bando, T.; Aihara, Y. *J. Chem. Phys.* **2002**, *117*, 5929−5939. (f) Aihara, Y.; Sugimoto, K.; Price, W. S.; Hayamizu, K. *J. Chem. Phys.* **2000**, *113*, 1981−1991. (g) Hayamizu, K.; Aihara, Y.; Arai, S.; Martinez, C. G. *J. Phys. Chem. B* **1999**, *103*, 519−524.

(4) (a) Garcia, B.; Lavallée, S.; Perron, G.; Michot, C.; Armand, M. *Electrochim. Acta* **2004**, *49*, 4583−4588. (b) Holzapfel, M.; Jost, C.; Novak, P. *Chem. Commun.* **2004**, 2098−2099.

(5) Sakaebe, H.; Matsumoto, H. *Electrochem. Commun.* **2003**, *5*, 594−598.

(6) Egashira, M.; Okada, S.; Yamaki, J.; Dri, D. A.; Bonadies, F.; Scrosati, B. *J. Power Sources* **2004**, *138*, 240−244.

(7) Seki, S.; Kobayashi, Y.; Miyashiro, H.; Ohno, Y.; Usami, A.; Mita, Y.; Kihira, N.; Watanabe, M.; Terada, N. *J. Phys. Chem. B* **2006**, *110*, 10228−10230.

(8) Seki, S.; Kobayashi, Y.; Miyashiro, H.; Ohno, Mita, Y.; Usami, A.; Terada, N.; Watanabe, M. *Electrochem. Solid-State Lett.* **2005**, *8*, A577−A578.

(9) Matsumoto, H.; Sakaebe, H.; Tatsumi, K. *J. Power Sources* **2005**, *146*, 45−50.

(10) (a) Hayashi, S.; Ozawa, R.; Hamaguchi, H. *Chem. Lett.* **2003**, *32*, 498−499. (b) Saha, S.; Hayashi, S.; Kobayashi, A.; Hamaguchi, H. *Chem. Lett.* **2003**, *32*, 740−741. (c) Ozawa, R.; Hayashi, S.; Saha, S.; Kobayashi, A.; Hamaguchi, H. *Chem. Lett.* **2003**, *32*, 948−949. (d) Holbrey, J. D.; Reichert, W. M.; Nieuwenhuyzen, M.; Johnston, S.; Seddon, K. R.; Rogers, R. D. *Chem. Commun.* **2003**, 1636−1637.

(11) Umebayashi, Y.; Fujimori, T.; Sukizaki, T.; Asada, M.; Fujii, K.; Kanzaki, R.; Ishiguro, S. *J. Phys. Chem. A* **2005**, *109*, 8976−8982.

(12) Fujii, K.; Kanzaki Takamuku, T.; Fujimori, T.; Umebayashi, Y.; Ishiguro, S. *J. Phys. Chem. B* **2006**, *110*, 8179−8183.

(13) Fujimori, T.; Fujii, K.; Kanzaki, R.; Chiba, K.; Yamamoto, H.; Umebayashi, Y.; Ishiguro, S. *J. Mol. Liq.* **2007**, *131*−*132*, 216−224.

(14) Lopes, J. N. A. C.; Padua, A. A. H. *J. Phys. Chem. B* **2006**, *110*, 7485−7489.

(15) Deetlefs, M.; Hardacre, C.; Nieuwenhuyzen, M.; Padua, A. A. H.; Sheppard, O.; Soper, A. K. *J. Phys. Chem. B* **2006**, *110*, 12055−12061.

(16) Herstedt, M.; Smirnov, M.; Johansson, P.; Chami, M.; Grondin, J.; Servant, L.; Lassègues, J. C. *J. Raman Spectrosc.* **2005**, *36*, 762−770.

(17) Herstedt, M.; Henderson, W. A.; Smirnov, M.; Ducasse, L.; Servant, L.; Talaga, D.; Lassègues, J. C. *J. Mol. Struct.* **2006**, *783*, 145−156.

(18) Kameda, Y.; Umebayashi, Y.; Takeuchi, M.; Wahab, M. A.; Fukuda, S.; Ishiguro, S.; Sasaki, M.; Amo, Y.; Usuk, T. *J. Phys. Chem. B* **2007**, *111*, 6104−6109.

(19) Matsumoto, K.; Hagiwara, R.; Tamada, O. *Solid State Sci.* **2006**, *8*, 1103−1107.

(20) (a) Castriota, M.; Caruso, T.; Agostino, R. G.; Cazzanelli, E.; Henderson, W. A.; Passerini, S. *J. Phys. Chem. A* **2005**, *109*, 92−96. (b) Nicotera, I.; Oliviero, C.; Henderson, W. A.; Appetecchi, G. B.; Passerini, S. *J. Phys. Chem. B* **2005**, *109*, 22814−22819.

(21) Borodin, O.; Smith; Henderson, W. *J. Phys. Chem. B* **2006**, *110*, 16879−16886.

(22) Hardwick, L. J.; Holzapfel, M.; Wokaun, A.; Novák, P. *J. Raman Spectrosc.* **2007**, *38*, 110−112.

(23) Lassègues, J.; Grondin, J.; Talaga, D. *Phys. Chem. Chem. Phys.* **2006**, *8*, 5629−5632.

(24) Marquardt, D. W. *J. Soc. Ind. Appl. Math.* **1963**, *11*, 431.

(25) Press, W. H.; Flannery, B. P.; Teukolsky, S. A.; Vetterling, W. T. *Numerical Recipes*; Cambridge University Press: Cambridge, U.K., 1989.

(26) Becke, A. D. *J. Chem. Phys.* **1993**, *98*, 5648.

(27) (a) Lee, C.; Yang, W.; Parr, R. G. *Phys. Rev. B* **1988**, *37*, 785. (b) Miehlich, B.; Savin, A.; Stoll, H.; Preuss, H. *Chem. Phys. Lett.* **1989**, *157*, 200.

(28) (a) Simon, S.; Duran, M.; Dannenberg, J. J. *J. Chem. Phys.* **1996**, *105*, 11024. (b) Boys, S. F.; Bernardi, F. *Mol. Phys.* **1970**, *19*, 553.

(29) Frisch, M. J.; Trucks, G. W.; Schlegel, H. B.; Scuseria, G. E.; Robb, M. A.; Cheeseman, J. R.; Montgomery, J. A., Jr.; Vreven, T.; Kudin, K. N.; Burant, J. C.; Millam, J. M.; Iyengar, S. S.; Tomasi, J.; Barone, V.; Mennucci, B.; Cossi, M.; Scalmani, G.; Rega, N.; Petersson, G. A.; Nakatsuji, H.; Hada, M.; Ehara, M.; Toyota, K.; Fukuda, R.; Hasegawa, J.; Ishida, M.; Nakajima, T.; Honda, Y.; Kitao, O.; Nakai, H.; Klene, M.; Li, X.; Knox, J. E.; Hratchian, H. P.; Cross, J. B.; Adamo, C.; Jaramillo, J.; Gomperts, R.; Stratmann, R. E.; Yazyev, O.; Austin, A. J.; Cammi, R.; Pomelli, C.; Ochterski, J. W.; Ayala, P. Y.; Morokuma, K.; Voth, G. A.; Salvador, P.; Dannenberg, J. J.; Zakrzewski, V. G.; Dapprich, S.; Daniels, A. D.; Strain, M. C.; Farkas, O.; Malick, D. K.; Rabuck, A. D.; Raghavachari, K.; Foresman, J. B.; Ortiz, J. V.; Cui, Q.; Baboul, A. G.; Clifford, S.; Cioslowski, J.; Stefanov, B. B.; Liu, G.; Liashenko, A.; Piskorz, P.; Komaromi, I.; Martin, R. L.; Fox, D. J.; Keith, T.; Al-Laham, M. A.; Peng, C. Y.; Nanayakkara, A.; Challacombe, M.; Gill, P. M. W.; Johnson, B.; Chen, W.; Wong, M. W.; Gonzalez, C.; Pople, J. A. *Gaussian 03*, revision B.04; Gaussian, Inc.: Pittsburgh, PA, 2003.

(30) (a) Rey, I.; Johansson, P.; Lindgren, J.; Lassègues, J. C.; Grondin, J.; Servant, L. *J. Phys. Chem. A* **1998**, *102*, 3249. (b) Huang, W.; Frech, R.; Wheeler, R. A. *J. Phys. Chem.* **1994**, *98*, 100. (c) Bakker, A.; Gejji, S.; Lindgren, J.; Hermansson, K.; Probst, M. M. *Polymer* **1995**, *36*, 4371.

(31) (a) Edman, L. *J. Phys. Chem. B* **2000**, *104*, 7254. (b) Rey, I.; Lassegues, J. C.; Grondin, J.; Servant, L. *Electrochim. Acta* **1998**, *43*, 1505.

(32) (a) Johansson, P.; Jacobsson, P. *J. Phys. Chem. A* **2001**, *105*, 8504−8509. (b) Gejji, S. P.; Suresh, C. H.; Babu, K.; Gadre, S. R. *J. Phys. Chem. A* **1999**, *103*, 7474−7480. (c) Arnaud, R.; Benrabah, D.; Sanchez, J.-Y. *J. Phys. Chem.* **1996**, *100*, 10882−10891.

(33) Tsuzuki, S.; Seki, S.; Hayamizu, K. Private communication.

(34) Olsher, U.; Izatt, R. M.; Bradshaw, J. S.; Dalley, N. K. *Chem. Rev.* **1991**, *91*, 137−164.

(35) Lassègues, J. C.; Grondin, J.; Holomb, R.; Johansson, P. *J. Raman Spectrosc.* **2007**, *38*, 551−558.

(36) Babai, A.; Mudring, A.-V. *Inorg. Chem.* **2006**, *45*, 3249.